Observational constraints on the spectral index of the cosmological curvature perturbation

David H. Lyth
Physics Department, Lancaster University, Lancaster LA1 4YB, Great Britain

Laura Covi
DESY Theory Group, Notkestrasse 85, D-22603 Hamburg, Germany
(Received 22 February 2000; published 6 October 2000)

We evaluate the observational constraints on the spectral index n, in the context of the ΛCDM hypothesis which represents the simplest viable cosmology. We first take n to be practically scale independent. Ignoring reionization, we find at a nominal 2-σ level $n \simeq 1.0 \pm 0.1$. If we make the more realistic assumption that reionization occurs when a fraction $f \sim 10^{-5}$ to 1 of the matter has collapsed, the 2-σ lower bound is unchanged while the 1-σ bound rises slightly. These constraints are compared with the prediction of various inflation models. Then we investigate the two-parameter scale-dependent spectral index, predicted by running-mass inflation models, and find that present data allow significant scale dependence of n, which occurs in a physically reasonable regime of parameter space.

PACS number(s): 98.80.Cq

I. INTRODUCTION

It is generally supposed that structure in the Universe originates from a primordial Gaussian curvature perturbation, generated by slow-roll inflation. The spectrum $\mathcal{P}_{\mathcal{R}}(k)$ of the curvature perturbation is the point of contact between observation and models of inflation. It is given in terms of the inflaton potential $V(\phi)$ by[1]

$$\frac{4}{25}\mathcal{P}_{\mathcal{R}}(k) = \frac{1}{75\pi^2 M_{\rm P}^6}\frac{V^3}{V'^2}, \tag{1}$$

where the potential and its derivatives are evaluated at the epoch of horizon exit $k=aH$. To work out the value of ϕ at this epoch one uses the relation

$$\ln(k_{\rm end}/k) \equiv N(k) = M_{\rm P}^{-2}\int_{\phi_{\rm end}}^{\phi}(V/V')\,{\rm d}\phi, \tag{2}$$

where $N(k)$ is actually the number of e-folds from the horizon exit to the end of slow-roll inflation. At the scale explored by the Cosmic Background Explorer (COBE) measurement of the cosmic microwave background (CMB) anisotropy, $N(k_{\rm COBE})$ depends on the expansion of the Universe after inflation in the manner specified by Eq. (30) below.

Given this prediction, the observed large-scale normalization $\mathcal{P}_{\mathcal{R}}^{1/2} \simeq 10^{-5}$ provides a strong constraint on models of inflation. Taking that for granted, we are here interested in the scale dependence of the spectrum, defined by the, in general, scale-dependent spectral index n:

$$n(k) - 1 \equiv \frac{{\rm d}\ln\mathcal{P}_{\mathcal{R}}}{{\rm d}\ln k}. \tag{3}$$

According to most inflation models, n has negligible variation on cosmological scales so that $\mathcal{P}_{\mathcal{R}} \propto k^{n-1}$, but we shall also discuss an interesting class of models giving a different scale dependence.

From Eqs. (1) and (2),

$$n - 1 = 2M_{\rm P}^2(V''/V) - 3M_{\rm P}^2(V'/V)^2, \tag{4}$$

and in almost all models of inflation, Eq. (4) is well approximated by

$$n - 1 = 2M_{\rm P}^2(V''/V). \tag{5}$$

We see that the spectral index measures the *shape* of the inflaton potential $V(\phi)$, being independent of its overall normalization. For this reason, it is a powerful discriminator between models of inflation.

The observational constraints on the spectral index have been studied by many authors, but a new investigation is justified for two reasons. On the observational side, the cosmological parameters are at last being pinned down, as is the height of the first peak in the spectrum the CMB anisotropy. No study has yet been given which takes on board these observational developments, while at the same time taking on board the crucial influence of the reionization epoch on the peak height. On the theory side, it is known that the spectral index may be strongly scale dependent if the inflaton has a gauge coupling, leading to what are called running-mass models. The quite specific, two-parameter prediction for the scale dependence of the spectral index in these models has not been compared with presently available data.

[1]As usual, $M_{\rm P} = 2.4 \times 10^{18}$ GeV is the Planck mass, a is the scale factor and $H = \dot{a}/a$ is the Hubble parameter, and k/a is the wave number. We assume the usual slow-roll conditions $M_{\rm P}^2|V''/V| \ll 1$ and $M_{\rm P}^2(V'/V)^2 \ll 1$, leading to $3H\dot{\phi} \simeq -V'$.

II. THE OBSERVATIONAL CONSTRAINTS ON THE PARAMETERS OF THE ΛCDM MODEL

Observations of various types indicate that we live in a low density Universe, which is at least approximately flat [1–5]. In the interest of simplicity we therefore adopt the cold dark matter model with a cosmological constant (ΛCDM model, defined by the requirements that the Universe is exactly flat, and that the non-baryonic dark matter is cold with negligible interaction. Essentially exact flatness is predicted by inflation, unless one invokes a special kind of model, or special initial conditions. Also, there is no clear motivation to modify the cold dark matter hypothesis.[2] We shall constrain the parameters of the ΛCDM model, including the spectral index, by performing a least-squares fit to key observational quantities.

A. The parameters

The ΛCDM model is defined by the spectrum $\mathcal{P}_{\mathcal{R}}(k)$ of the primordial curvature perturbation, and the four parameters that are needed to translate this spectrum into spectra for the matter density perturbation and the CMB anisotropy. The four parameters are the Hubble constant h (in units of $100\ \mathrm{km\,s^{-1}\,Mpc^{-1}}$), the total matter density parameter Ω_0, the baryon density parameter $\Omega_{\rm b}$, and the reionization redshift $z_{\rm R}$. As we shall describe, $z_{\rm R}$ is estimated by assuming that reionization occurs when some fixed fraction f of the matter collapses. Within the reasonable range $f\sim 10^{-4}$ to 1, the main results are insensitive to the precise value of f.

The spectrum is conveniently specified by its value at a scale explored by COBE, and the spectral index $n(k)$. We shall consider the usual case of a constant spectral index, and the case of running mass models where $n(k)$ is given by a two-parameter expression. Since $\mathcal{P}_{\mathcal{R}}(k_{\rm COBE})$ is determined very accurately by the COBE data [Eq. (15) below] we fix its value. Excluding $z_{\rm R}$ and $\mathcal{P}_{\mathcal{R}}(k_{\rm COBE})$, the Λ CDM model is specified by four parameters in the case of a constant spectral index, or by five parameters in the case of running mass inflation models.

B. The data

To compare the ΛCDM model with observation, we take as our starting point a study performed a few years ago [7]. We consider the same seven observational quantities as in the earlier work, since they still summarize most of the relevant data. Of these quantities, three are the cosmological quantities h, Ω_0, $\Omega_{\rm B}$, which we are also taking as free parameters. The crucial difference between the present situation and the earlier one is that observation is beginning to pin down h and Ω_0. Judging by the spread of measurements, the systematic error, while still important, is no longer completely dominant compared with the random error. At least at some crude level, it therefore makes sense to pretend that the errors are all random, and to perform a least squares fit. The adopted values and errors are given in Table I, and summarized below. In common with earlier investigations, we take the errors to be uncorrelated.

(a) *Hubble constant*. On the basis of observations that have nothing to do with large scale structure it seems very likely [1] that h is in the range 0.5 to 0.8. We therefore adopt, at notionally the 2-σ level, the value $h=0.65\pm 0.15$, corresponding to $h=0.65\pm 0.075$ at the notional 1-σ level.

(b) *The matter density*. The case of the total density parameter Ω_0 is similar to that of the Hubble parameter. On the basis of observations that have nothing to do with large scale structure, it seems very likely [1] that Ω_0 lies between 0.2 and 0.5, and we adopt at the notional 1-σ level the value $\Omega_0=0.35\pm 0.075$.

(c) *The baryon density*. As described for instance in [8,9], the baryon density parameter $\Omega_{\rm b}$ has two likely ranges. At the 1-σ level, these are estimated in [8] to be $\Omega_{\rm b}h^2=.019\pm.002$ and $\Omega_{\rm b}h^2=.007\pm.0015$. We adopt the high $\Omega_{\rm b}$ range, which is generally regarded as the most likely, though our conclusions would be much the same if we were to adopt the low range.

(d) *The rms density perturbation at $8h^{-1}\,Mpc$*. Primarily through the abundance of rich galaxy clusters, a useful constraint on the primordial spectrum is provided by the rms density contrast, in a comoving sphere with present radius $R\sim 10h^{-1}\,\mathrm{Mpc}$, at redshift $z=0$ to a few. The constrained quantity is conventionally taken to be the present, linearly evolved rms density contrast at $R=8h^{-1}\,\mathrm{Mpc}$, denoted by σ_8. A recent estimate [10] based on low-redshift clusters gives at 1-σ

$$\sigma_8=\tilde{\sigma}_8\Omega_0^{-0.47} \tag{6}$$

$$\tilde{\sigma}_8=.560\pm.059. \tag{7}$$

This constrains the primordial curvature perturbation on the scale $k\sim k_8\equiv(8h^{-1}\,\mathrm{Mpc})^{-1}$.

(e) *The shape parameter*. The slope of the galaxy correlation function on scales of order $1h^{-1}$ to $100h^{-1}\,\mathrm{Mpc}$ is conveniently specified by a shape parameter [7] $\tilde{\Gamma}$, defined by

$$\tilde{\Gamma}=\Gamma-0.28(n_8^{-1}-1) \tag{8}$$

$$\Gamma=\Omega_0 h\ \exp(-\Omega_{\rm B}-\Omega_{\rm B}/\Omega_0). \tag{9}$$

(The quantity Γ determines, to an excellent approximation, the shape of the matter transfer function on scales $k^{-1}\sim 1$ to $100h^{-1}\,\mathrm{Mpc}$, while the second term accounts for the scale dependence of the primordial spectrum. For definiteness, we evaluate n at $k=k_8$, in the case that n has significant scale dependence.) A fit reported in [7] gives $\tilde{\Gamma}=.23$ with a 15% uncertainty at 2-σ. A more recent fit with more data [11] gives $\tilde{\Gamma}=.20$ to .25, depending on the assumed velocity dis-

[2]In particular, the rotation curves of dwarf galaxies may be compatible with cold dark matter [6].

persion, but with 15% statistical uncertainty at the 1-σ level.[3] We therefore adopt $\tilde{\Gamma}=.23$, with 15% uncertainty at 1-σ.

(f) *The COBE normalization of the spectrum*. To a good approximation, the spectrum C_l of the CMB anisotropy at large l is sensitive to the primordial spectrum on the corresponding scale at the particle horizon,

$$k(l,\Omega_0)=\frac{l}{x_{\rm hor}(\Omega_0)} \tag{10}$$

$$x_{\rm hor}\equiv 2H_0^{-1}\Omega_0^{-1/2}(1+0.084\ln\Omega_0). \tag{11}$$

The COBE measurements cover the range $2\leqslant l\lesssim 30$, and they constrain $\mathcal{P}_{\mathcal{R}}(k)$ on the corresponding scales. Instead of $\mathcal{P}_{\mathcal{R}}$, it is usual in this context to consider a quantity δ_H, which is of direct interest for studies of structure formation and is defined by

$$\delta_H(k)\equiv\frac{2}{5}\frac{g(\Omega_0)}{\Omega_0}\mathcal{P}_{\mathcal{R}}{}^{1/2}(k) \tag{12}$$

$$g(\Omega_0)\equiv\frac{5}{2}\Omega_0\left(\frac{1}{70}+\frac{209\Omega_0}{140}-\frac{\Omega_0^2}{140}+\Omega_0^{4/7}\right)^{-1}. \tag{13}$$

The factor g/Ω_0, normalized to 1 at $\Omega_0=1$, represents the Ω_0 dependence of the present, linearly evolved, density contrast after pulling out the scale-dependent transfer function and $\mathcal{P}_{\mathcal{R}}$. Equivalently, $a(\Omega)g(\Omega)$ is the time dependence of the density contrast after matter domination.

According to the ordinary (as opposed to ''integrated'') Sachs-Wolfe approximation

$$C_l=\frac{4\pi}{25}\int_0^\infty\frac{{\rm d}k}{k}j_l^2(kx_{\rm hor})\mathcal{P}_{\mathcal{R}}(k). \tag{14}$$

In the regime $l\gg 1$, it satisfies Eq. (10) because j_l^2 peaks when its argument is equal to l. In the ΛCDM model, the Sachs-Wolfe approximation is quite good in COBE regime, but still the quality of the data justify using the full (linear) calculation, given for instance by the output of the CMBFAST package [12].

Consider first the case $n=1$ (scale-independent spectrum). In the Sachs-Wolfe approximation, the value of $\mathcal{P}_{\mathcal{R}}$ obtained by fitting the COBE data is independent of the cosmological parameters h, Ω_0 and $\Omega_{\rm b}$. Using instead the full calculation, a fit to the data by Bunn and White [13] gives

$$\delta_H=\Omega_0^{-0.785-0.05\ln\Omega_0}\tilde{\delta}_H$$

$$10^5\tilde{\delta}_H=1.94\pm 0.08. \tag{15}$$

[3]See Table III of [11]; in the present context one should focus on the last three rows of the table.

As expected, the corresponding spectrum of the curvature perturbation has only mild dependence on Ω_0 ($\mathcal{P}_{\mathcal{R}}\propto\Omega_0^{-0.03}$).

Consider next the case of a scale-independent spectral index $n\neq 1$. Dropping an insignificant term quadratic in $n-1$, the fit of Bunn and White [13] handles the n-dependence by assuming that Eq. (15) holds at a ''pivot'' scale $k_{\rm COBE}$ which is independent of Ω_0,[4]

$$k_{\rm COBE}\equiv 6.6H_0 \tag{16}$$

Insofar as the approximation Eq. (10) is valid, this corresponds to fixing C_l at an Ω_0-dependent value of l, which is $l=13$ for Ω_0, and $l=22$ for our central value $\Omega_0=.35$.

In the case of a scale-independent n, an alternative fit is provided by the CMBFAST package, which chooses $\mathcal{P}_{\mathcal{R}}(k)$ to fit an n-independent best-fit value of C_{10}. As expected, the output of CMBFAST is in good agreement with the Bunn-White fit. Even better agreement is obtained using

$$k_{\rm COBE}(\Omega_0)\equiv 13.2/x_{\rm hor}, \tag{17}$$

which reduces to Eq. (16) for $\Omega_0=1$. Insofar as Eq. (10) is valid, this Ω_0-dependent pivot for k corresponds to an Ω_0-independent pivot for l, namely $l=13$.

We are also interested in the scale-dependent n predicted by the running-mass inflation models. However, as the range of scales explored by COBE corresponds to only $\Delta N\simeq 2$, with the central values of l the most important, we can take the variation of n to be negligible on these scales.

Guided by these considerations, we have adopted three slightly different versions of the COBE normalization, chosen for convenience according to the context. When calculating $\tilde{\Gamma}$ and $\tilde{\sigma}_8$, we in all cases fixed δ_H at the central value given by Eq. (15), at the Bunn-White pivot point $k_{\rm COBE}$. When calculating the height of the first peak in the CMB anisotropy, in the case of the running-mass model, we used Eq. (10), with δ_H again fixed at the central value given by Eq. (15) but now evaluated at the slightly more accurate pivot point $k_{\rm COBE}(\Omega_0)$. Finally, when evaluating the peak height in the case of scale-independent n, we used a linear fit to the output of CMBFAST. Explicit expressions for the peak height will be given after considering the effect of reionization.

(g) *The peak height*. The model under consideration predicts a peak in the CMB anisotropy at $l\simeq 210$ to 230, and presently available data [2–5] confirm the existence of a peak at about this position. We adopt as a crucial observational quantity $\tilde{C}_{\rm peak}$, defined as the maximum value of

$$\tilde{C}_l\equiv l(l+1)C_l/2\pi. \tag{18}$$

[4]Keeping the quadratic term, the ''pivot'' scale at which Eq. (15) holds is dependent on n, but still independent of Ω_0. A related fit by Bunn, Liddle and White [14] keeps a cross term in $(n-1)$ and Ω_0, which makes the ''pivot'' scale increase with Ω_0^{-1}, though not as strongly as in Eq. (17) below.

Presently available data give conflicting estimates [2–5] of $\sqrt{\tilde{C}_{\rm peak}}$, with central values in the range 70 to 90 μK. We adopt (80 ± 10) μK with the uncertainty taken to be at 1-σ.

C. Reionization

The effect of reionization on the CMB anisotropy is determined by the optical depth τ. We assume sudden, complete reionization at redshift $z_{\rm R}$, so that the optical depth τ is given by [15,16]

$$\tau = 0.035 \frac{\Omega_{\rm b}}{\Omega_0} h(\sqrt{\Omega_0(1+z_{\rm R})^3+1-\Omega_0}-1). \qquad (19)$$

In previous investigations, $z_{\rm R}$ has been regarded as a free parameter, usually fixed at zero or some other value. In this investigation, we instead take on board that fact that $z_{\rm R}$ can be estimated, in terms of the parameters that we are varying plus assumed astrophysics. Indeed, it is usually supposed that reionization occurs at an early epoch, when some fraction f of the matter has collapsed, into objects with mass very roughly $M=10^6 M_\odot$. Estimates of f are in the range [17]

$$10^{-4.4} \lesssim f \lesssim 1. \qquad (20)$$

In the case $f \ll 1$, the Press-Schechter approximation gives the estimate

$$1+z_{\rm R} \simeq \frac{\sqrt{2}\sigma(M)}{\delta_{\rm c} g(\Omega_0)} \,{\rm erfc}^{-1}(f) \;\; (f \ll 1). \qquad (21)$$

Here $\sigma(M)$ is the present, linearly evolved, rms density contrast with top-hat smoothing, and $\delta_{\rm c}=1.7$ is the overdensity required for gravitational collapse. (g is the suppression factor of the linearly evolved density contrast at the present epoch, which does not apply at the epoch of reionization.) In the case $f \sim 1$, one can justify only the rough estimate

$$1+z_{\rm R} \sim \frac{\sigma(M)}{g(\Omega_0)} \;\; (f \sim 1). \qquad (22)$$

[This estimate is not very different from the one that would be obtained by using $f=1$ in Eq. (21).]

In our fits, we fix f at different values in the above range, and find that the most important results are not very sensitive to f even though the corresponding values of $z_{\rm R}$ can be quite high.

D. The predicted peak height

The CMBFAST package [12] gives C_l, for given values of the parameters with n taken to be scale-independent. Following [18], we parameterize the CMBFAST output at the first peak in the form

$$\sqrt{\tilde{C}_{\rm peak}} = \sqrt{\tilde{C}^{(0)}_{\rm peak}} \left(\frac{220}{10}\right)^{\nu/2}, \qquad (23)$$

where

$$\nu \equiv a_n(n-1) + a_h \ln(h/0.65) + a_0 \ln(\Omega_0/0.35) + a_{\rm b} h^2 (\Omega_{\rm b} - \Omega_{\rm b}^{(0)}) - 0.65 f(\tau)\tau. \qquad (24)$$

$\sqrt{\tilde{C}^{(0)}_{\rm peak}}$ is the value of $\sqrt{\tilde{C}_{\rm peak}}$ evaluated with each term of ν equal to zero. The coefficients for the high choice $\Omega_{\rm b}^{(0)} h^2 = 0.019$ are $a_n = 0.88$, $a_h = -0.37$, $a_0 = -0.16$, $a_{\rm b} = 5.4$, and $\sqrt{\tilde{C}^{(0)}_{\rm peak}} = 77.5$ μK. The formula reproduces the CMBFAST results within 10% for a 1-σ variation of the cosmological parameters, h, Ω_0 and $\Omega_{\rm b}$, and $n_{\rm COBE} = 1.0 \pm 0.05$. With the function $f(\tau)$ set equal to 1, the term -0.65τ is equivalent to multiplying $\sqrt{\tilde{C}_{\rm peak}}$ by the usual factor $\exp(-\tau)$. We use the following formula, which was obtained by fitting the output of CMBFAST, and is accurate to a few percent over the interesting range of τ:

$$f = 1 - 0.165\tau/(0.4+\tau). \qquad (25)$$

For the running-mass model, we start with the above estimate for $n=1$, and adjust it using Eq. (10). Adopting the COBE normalization mentioned earlier, this adjustment is

$$\frac{\sqrt{\tilde{C}_{\rm peak}}}{\sqrt{\tilde{C}^{(n=1)}_{\rm peak}}} = \frac{\delta_H[k(l,\Omega_0)]}{\delta_H[k_{\rm COBE}(\Omega_0)]}. \qquad (26)$$

In the case of constant n, this prescription corresponds to the previous one with $a_n = 0.91$, in good agreement with the output of CMBFAST.

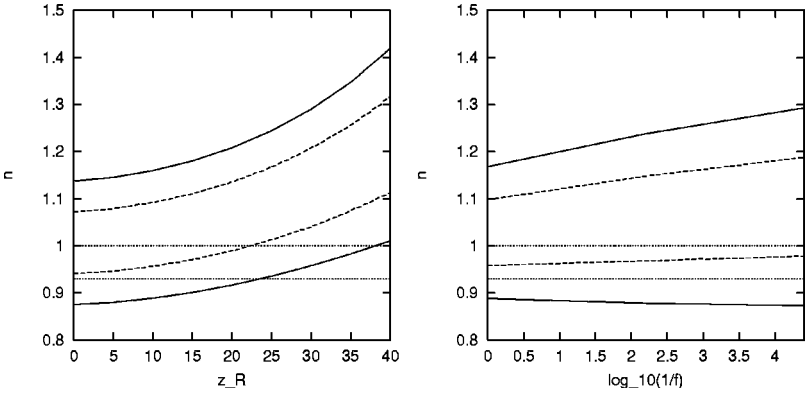

FIG. 1. The nominal 1- and 2-σ bounds on n. In the left-hand panel, the reionization redshift $z_{\rm R}$ is fixed. In the right-hand panel, reionization is assumed to occur when a fixed fraction f of matter collapses (corresponding reionization redshift, not shown, is roughly in the range 10 to 35). A result $n>1$ would rule out most known models of inflation, a result $n>.93$ would rule out ''new'' inflation with a cubic potential; these cases are indicated by horizontal lines.

TABLE I. Fit of the ΛCDM model to presently available data, with $z_R=20$. The spectral index n is a parameter of the model, and so are the next three quantities. Every quantity except n is a data point, with the value and uncertainty listed in the first two rows. The result of the least-squares fit is given in the lines three to five. All uncertainties are at the nominal 1-σ level. The total χ^2 is 1.8 for two degrees of freedom.

	n	$\Omega_b h^2$	Ω_0	h	$\tilde{\Gamma}$	$\tilde{\sigma}_8$	$\sqrt{\tilde{C}_{peak}}$
data	—	0.019	0.35	0.65	0.23	0.56	80 μK
error	—	0.002	0.075	0.075	0.035	0.059	10 μK
fit	1.064	0.019	0.34	0.63	0.19	0.59	77 μK
error	0.077	0.002	0.06	0.06	—	—	—
χ^2	—	9×10^{-5}	3×10^{-2}	0.1	1.3	0.2	0.1

III. CONSTANT SPECTRAL INDEX

A. The observational constraints

Most models of inflation make n roughly scale-independent, over the cosmologically interesting range. We therefore begin by considering the case that n is exactly scale-independent. The resulting bound on n is shown in Fig. 1. In the left-hand panel we make the traditional assumption that reionization occurs at some fixed redshift z_R. In the right-hand panel we make the more reasonable assumption, that it occurs when some fixed fraction f of the matter collapses, in a reasonable range $10^{-4.5}<f<1$. The bounds in the latter case are relatively insensitive to f, because the corresponding range of z_R is narrower; everywhere on the displayed curves, z_R is within (usually well within) the range 8 to 36. Details of the fit for $z_R=20$ are given in Table I. Practically the same fit is obtained if instead we fix f at $10^{-1.9}$.

The least-squares fits were performed with the CERN MINUIT package, and the quoted error bars invoke the usual parabolic approximation (i.e., it they are the diagonal elements of the error matrix). The exact error bars given by the same package agree to better than 10%. For z_R, our results are similar to those obtained in [19], but more precise because of improvements in our knowledge of the cosmological parameters; they are also similar to those obtained in [20], if we take the errors to be the ones given by the error matrix. (We do not know why the exact error bars in [20] are about three times bigger, in conflict with both our work and that of [19].)

After we completed this work, the BOOMeranG [3] and MAXIMA [5] measurements of the CMB anisotropy appeared, both of which extend to the second acoustic peak. Fits to these data [21,22] seem to again give a similar constraint on n, but the values for Ω_b, Ω_c and h outside our adopted 2-σ range. At the time of writing, the new CMB data have not been included in a fit of the type that we are performing (i.e., with with strong prior requirements on the cosmological parameters, as well as on the small-scale data $\tilde{\sigma}_8$ and $\tilde{\Gamma}$).

B. Models of inflation giving $n<1$

Although the quality and quantity of data are insufficient for a proper statistical analysis, these bounds on n are very striking when compared with theoretical expectations. These expectations [23,16] are summarized[5] in Tables II and III, and we now discuss them beginning with the usual case $n<1$ (red spectrum). Details of the models and references are given in [23].

TABLE II. Predictions for the spectral index $n(k)$. Wave number k is related to number of e-folds N by $d\ln k=-dN$. Constants q and Q are positive, and p can have either sign.

Comments	$V(\phi)/V_0$	$\frac{1}{2}(n-1)$
Mass term	$1\pm\frac{1}{2}\frac{m^2}{V_0}\phi^2$	$\pm M_P^2 m^2/V_0$
p integer $\leqslant -1$ or $\geqslant 3$	$1+\lvert c\rvert\phi^p$	$\frac{p-1}{p-2}\frac{1}{N_{max}-N}$
Spont. broken SUSY	$1+\lvert c\rvert\ln\frac{\phi}{Q}$	$-\frac{1}{2N}$
Various models	$1-e^{-q\phi}$	$-\frac{1}{N}$
$p>2$ or $-\infty<p<1$	$1-\lvert c\rvert\phi^p$	$-\left(\frac{p-1}{p-2}\right)\frac{1}{N}$

The simplest prediction is for a potential of the form[6]

$$V=V_0-\frac{1}{2}m^2\phi^2+\cdots, \tag{27}$$

leading to $n-1=-2M_P^2m^2/V_0$. This is the form that one expects if ϕ is a string modulus (modular inflation), or a pseudo-Goldstone boson (natural inflation), or the radial part of a massive field spontaneously breaking a symmetry (topo-

[5]In the case of the power-law potentials (second and last lines of Table II), the stated prediction for n assumes that the field value is smaller than the Planck scale, which in some cases is a non-trivial restriction. With this restriction, all of the exhibited potentials generate gravitational waves with negligible amplitude. We do not consider the opposite case, of power-law potentials in which the field value is Planckian and significant gravitational waves may be generated, because the potential is then sensitive to non-renormalizable terms whose form is essentially arbitrary. In particular, we do not consider the ''chaotic inflation'' potentials $V\propto\phi^p$, which give $n-1=-(2+p)/(2N)$ with a significant gravitational contribution to the CMB anisotropy. Another restriction is that we do not consider ''two-field'' models, in which there is a family of inflaton trajectories; these models usually involve large fields, and with fine-tuning they can give a sharp feature in the spectrum. However, a recently-proposed two-field model [24] with small field values gives $(n-1)/2=-2/N$, which is the same as the prediction of the last line of Tables II and III with $p=3$.) Finally, we do not consider models based on non-Einstein gravity, which again usually involve large field values; one of them gives the exponential potential in Table II, with the corresponding prediction for N.

[6]In this expression and in Eqs. (28) and (35), the remaining terms are supposed to be negligible, and V_0 is supposed to dominate, while cosmological scales leave the horizon.

TABLE III. Predictions for the spectral index n, for some potentials of the form $V_0(1+c\phi^p)$ with *negative* c. The case $p\to 0$ corresponds to the potential $V_0(1+c\ln(\phi/Q))$, and the case $p\to-\infty$ corresponds to $V_0(1-e^{-q\phi})$. The parameter $N_{\rm COBE}<60$ depends on the cosmology after inflation.

p	n	
	$N_{\rm COBE}=50$	$N_{\rm COBE}=20$
$p\to 0$	0.98	0.95
$p=-2$	0.97	0.93
$p\to\pm\infty$	0.96	0.90
$p=4$	0.94	0.85
$p=3$	0.92	0.80

logical inflation). The vacuum expectation value (VEV) of ϕ in these models is expected to be of order $M_{\rm P}$ or less, while the potential Eq. (27) gives $\langle\phi\rangle\sim(1-n)^{-1/2}M_{\rm P}$. Therefore, the present bound $n\gtrsim 0.9$ is already beginning to disfavor these models. The potential Eq. (27) may however give n very close to 1 if the potential steepens after cosmological scales leave the horizon, for instance in an inverted hybrid inflation model.

Of the remaining models of Table II, those giving a red spectrum involve a potential basically of the form

$$V=V_0(1+c\phi^p+\cdots), \tag{28}$$

with c *negative* and p *not* in the range $1\leqslant p\leqslant 2$. (''New'' inflation corresponds to p an integer $\geqslant 3$, while mutated hybrid inflation models account for the rest of the range. The logarithmic and exponential potentials in Table II may be regarded as the limits respectively $p\to 0$ and $p\to-\infty$.) With this form, the prediction is

$$n-1=-\left(\frac{p-1}{p-2}\right)\frac{2}{N}. \tag{29}$$

For the moment, we ignore the mild scale dependence and set $N=N_{\rm COBE}$.

Depending on the history of the Universe,

$$N_{\rm COBE}\simeq 60-\ln(10^{16}\,{\rm GeV}/V^{1/4})-\frac{1}{3}\ln(V^{1/4}/T_{\rm reh})-N_0. \tag{30}$$

In this expression, $T_{\rm reh}$ is the reheat temperature, while the final contribution $-N_0$ (negative in all reasonable cosmologies) encodes our ignorance about what happens between the end of inflation and nucleosynthesis. Let us pause to discuss this ignorance. In the present context, we are defining $T_{\rm reh}$ as the temperature when the Universe *first* becomes radiation dominated after inflation. In the conventional cosmology, radiation domination persists until the present matter dominated era begins, long after nucleosynthesis. If this is the case, and if also slow-roll inflation gives way promptly to matter domination as is the case in most models, then $N_0=0$.[7] In this conventional case, $N_{\rm COBE}$ is largely determined by $V_0^{1/4}$, and hence by the model of inflation. It is certainly in the range 32 to 60 (lower limit corresponding to $V_0^{1/4}=100\,{\rm GeV}$) and much more likely in the range 40 to 60 (lower limit corresponding to $V_0^{1/4}\sim 10^{10}\,{\rm GeV}$ and $T_{\rm reh}\sim 100\,{\rm GeV}$).

However, the conventional cosmology need not be correct. In particular, the initial radiation-dominated era may give way to matter domination by a late-decaying particle, and most crucially there may be an era of thermal inflation [25] during the transition. This unconventional cosmology, with its huge entropy dilution after inflation, is indeed demanded in many inflation models, if gravitinos created from the vacuum fluctuation [26] persists to late times [27]. Even one bout of thermal inflation will give $N_0\sim 10$ and additional bout(s) cannot be ruled out. Thus, from the theoretical viewpoint, $N_{\rm COBE}$ can be anywhere in the range 0 to 60.

Let us discuss the prediction Eq. (29), excluding for simplicity the ranges $0<p<1$ and $2<p<3$ (recall that the straightforward ''new'' inflation models make p an integer $\geqslant 3$). Taking the maximum value $N_{\rm COBE}\simeq 60$, we learn that $n<0.93$ for $p=3$ (the lowest prediction), and $n<0.95$ for $p=4$. Looking at the right-hand panel of Fig. 1, we see that at nominal 1-σ level, the former case is ruled out, though it is still allowed at the 2-σ level. Stronger results hold if $N_{\rm COBE}<60$. Looking at things another way, a lower bound on n gives a lower bound on $N_{\rm COBE}$,

$$N_{\rm COBE}>\frac{p-1}{p-2}\,\frac{2}{1-n}. \tag{31}$$

Even with present data, the 2-σ result $n\gtrsim .9$ gives $N_{\rm COBE}\gtrsim 40$ for $p=3$, and $N_{\rm COBE}\gtrsim 20$ for $p\gg 3$.

The scale dependence given by Eq. (29) is

$$\frac{{\rm d}n}{{\rm d}\ln k}=-\frac{1}{2}\left(\frac{p-2}{p-1}\right)(n-1)^2<0. \tag{32}$$

Over the cosmological range of scales $\ln(k/k_{\rm COBE})$ is at most a few, and in particular $\ln(8^{-1}h\,{\rm Mpc}^{-1}/k_{\rm COBE})\simeq 4$, corresponding to

$$\Delta n\equiv n_8-n_{\rm COBE}=-.02\left(\frac{p-2}{p-1}\right)\left(\frac{n-1}{0.1}\right)^2<0. \tag{33}$$

Taking $n=0.9$ to saturate the present bound, this gives $|\Delta n|<0.02$ with $p\geqslant 3$, and $|\Delta n|<0.04$ with $p\leqslant 0$. Even in the latter case, the change in n is hardly significant with present data.

[7] In some inflation models, slow-roll is followed by an extended era of fast-roll giving N_0 of order a few; for simplicity we ignore that possibility in the present discussion.

C. Models giving $n>1$

Known models giving $n>1$ (blue spectrum) are all of the hybrid inflation type. The simplest case is $V=V_0+\frac{1}{2}m^2\phi^2$; it gives the scale-independent prediction $n-1=2M_{\rm P}^2m^2/V_0$, which may be either close to 1 or well above 1.

The other cases involve a potential of the form $V=V_0(1+c\phi^p)$ with *positive* c, and p an integer $\geqslant 3$ or $\leqslant -1$. There is a maximum (early-time) value for N, and the prediction

$$n-1=\frac{p-1}{p-2}\frac{1}{N_{\rm max}-N}. \tag{34}$$

Barring the fine-tuning $N_{\rm COBE}\simeq N_{\rm max}$, this gives $n-1\ll 0.04$, which is compatible with the observational bound. The scale dependence of n in these models is still given by Eqs. (32) and (33); it may be observationally significant only in the fine-tuned case $N_{\rm COBE}\simeq N_{\rm max}$, which we have not investigated.

IV. THE RUNNING MASS MODELS

A. The potential

We have also done fits with the scale-dependent spectral index, predicted in inflation models with a running inflaton mass [28–33]. In these models, based on softly broken supersymmetry, one-loop corrections to the tree-level potential are taken into account, by evaluating the inflaton mass-squared $m^2(\ln(Q))$ at the renormalization scale $Q\simeq\phi$,[8]

$$V=V_0+\frac{1}{2}m^2(\ln(Q))\phi^2+\cdots. \tag{35}$$

Over any small range of ϕ, it is a good approximation to take the running mass to be a linear function of $\ln\phi$. This is equivalent to choosing the renormalization scale to be within the range, and then adding the loop correction explicitly,

$$V=V_0+\frac{1}{2}m^2(\ln Q)\phi^2-\frac{1}{2}c(\ln Q)\frac{V_0}{M_{\rm P}^2}\phi^2\ln(\phi/Q). \tag{36}$$

The dimensionless quantity c specifies the strength of the coupling. Let us discuss its likely magnitude, taking for definiteness $Q=\phi_{\rm COBE}$.

It has been shown [31] that the linear approximation is very good over the range of ϕ corresponding to horizon exit for scales between $k_{\rm COBE}$ and $8h^{-1}$ Mpc. We shall want to estimate the reionization epoch, which involves a scale of order $k_{\rm reion}^{-1}\sim 10^{-2}$ Mpc (enclosing the relevant mass of order $10^6M_\odot$). Since only a crude estimate of the reionization epoch is needed, we shall assume that the linear approximation is adequate down to this ''reionization scale.'' In other words, we assume that it is adequate for ϕ between $\phi_{\rm COBE}$ and $\phi_{\rm reion}$, the subscripts denoting the value of ϕ when the relevant scale leaves the horizon. Within this range, we it is convenient to write Eq. (37) in the form [31]

$$V=V_0-\frac{1}{2}\frac{V_0}{M_{\rm P}^2}c\phi^2\left(\ln\frac{\phi}{\phi_*}-\frac{1}{2}\right), \tag{37}$$

so that

$$V'=-\frac{V_0}{M_{\rm P}^2}c\phi\ln\frac{\phi}{\phi_*}. \tag{38}$$

In these expressions, the constants c and ϕ_* both depend on the renormalization scale Q, which can be chosen anywhere in the range corresponding to cosmological scales (say $Q=\phi_{\rm COBE}$). The dimensionful constant ϕ_* is related to the mass-squared by

$$\ln(\phi_*/Q)=\frac{m^2(Q)M_{\rm P}^2}{c(Q)V_0}-\frac{1}{2}. \tag{39}$$

Note that the limit of no running, $c\to 0$, corresponds to finite $c|\ln(\phi/\phi_*)|$, so that Eq. (37) in that limit gives back Eq. (35) with a constant mass.

In general, the point $\phi=\phi_*$ may be far outside the regime where the linear approximation Eq. (37) applies. However, in simple models the cosmological regime is sufficiently close to that point that the linear approximation is approximately valid there. In that case, we can trust the Eq. (37) and its derivatives for $\phi=\phi_*$; since V' vanishes at that point, there are four clearly distinct models of inflation as shown in Fig. 2. The labeling (i), (ii), (iii) and (iv) is the one introduced in [31]. In models (i) and (ii), c is positive and the potential has a maximum near ϕ_*, while in models (iii) and (iv), c is negative and there is a minimum. In models (i) and (iv), ϕ moves towards the origin, while in models (ii) and (iii) the opposite is true. Even if Eq. (37) is not valid near $\phi=\phi_*$, this fourfold classification of models, according to the sign of c and the direction of motion of ϕ, is still useful.

Let us discuss the likely magnitude of c, assuming that a single coupling dominates the loop correction. The value of c is conveniently obtained from the well-known RGE for $dm^2/d(\ln Q)$. If a gauge coupling dominates one finds [29]

$$\frac{V_0c}{M_{\rm P}^2}=\frac{2C}{\pi}\alpha\tilde{m}^2. \tag{40}$$

Here, C is a positive group-theoretic number of order 1, α is the gauge coupling, and $\tilde{m}$ is the gaugino mass. We see that *if the loop correction comes from a single gauge coupling, c is positive*, corresponding to model (i) or model (ii). If a Yukawa coupling dominates, one finds [32] (for negligible supersymmetry breaking trilinear coupling)

[8]The choice $Q\simeq\phi$ is to be made in the regime where ϕ is bigger than the relevant masses. When Q falls below the relevant masses, $m^2(Q)$ becomes practically scale-independent (the mass ''stops running''). We have a running mass model if inflation takes place in the former regime, which happens in some interesting cases [31,32], including that of a gauge coupling.

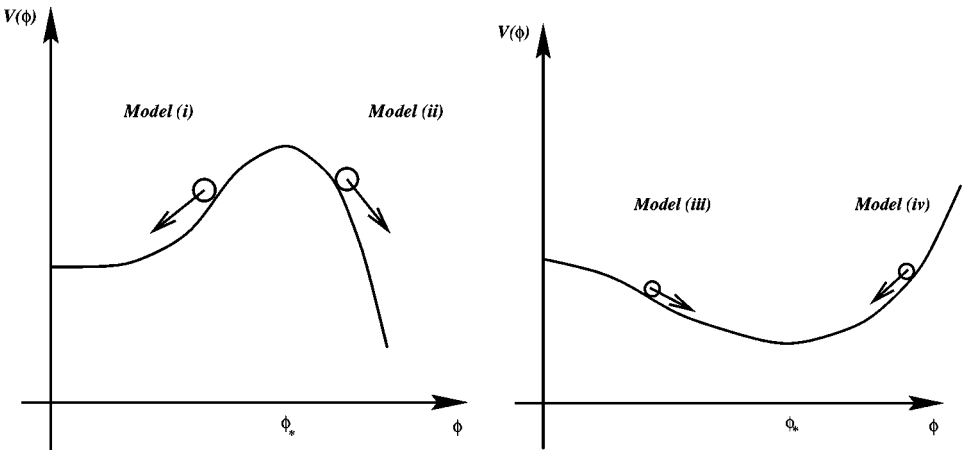

FIG. 2. Sketches of the potential for the different models in the case an extremum exists: the right panel shows the inflaton behavior for models (i) and (ii), while the left panel shows models (iii) and (iv).

$$\frac{V_0 c}{M_{\rm P}^2} = -\frac{D}{16\pi^2}|\lambda|^2 m_{loop}^2, \tag{41}$$

where D is a positive constant counting the number of scalar particles interacting with the inflaton, $m_{\rm loop}^2$ is their common SUSY breaking mass-squared, and λ is their common Yukawa coupling. In this case, c can be of either sign.

To complete our estimate of c, we need the gaugino or scalar mass. The traditional hypothesis is that soft supersymmetry breaking is gravity-mediated, and in the context of inflation this means that the scale $M_{\rm S}$ of supersymmetry breaking will be roughly $V_0^{1/4}$. (As usual we are defining $M_{\rm S} \equiv \sqrt{F}$, where F is the auxiliary field responsible for spontaneous supersymmetry breaking in the hidden sector. We also assume that there is no accurate cancelation in the formula $V = |F|^2 - 3M_{\rm P}^2 m_{3/2}^2$, which is the case in most supersymmetric inflation models [23].) With gravity-mediated SUSY breaking, typical values of the masses are $\tilde{m}^2 \sim |m_{\rm loop}^2| \sim V_0/M_{\rm P}^2$, which makes $|c|$ of order of the coupling strength α or $|\lambda|^2$. At least in the case of a gauge coupling, one then expects

$$|c| \sim 10^{-1} \ \text{ to } \ 10^{-2}. \tag{42}$$

In special versions of gravity-mediated SUSY breaking, the masses could be much smaller, leading to $|c| \ll 1$. In that case, the mass would hardly run, and the spectral index would be practically scale-independent. With gauge-mediated SUSY breaking, the masses could be much bigger; this would not lead to a model of inflation (unless the coupling is suppressed) because it would not satisfy the slow-roll requirement $|c| \lesssim 1$.

B. The spectrum and the spectral index

Using Eq. (2) we find

$$s e^{c\Delta N(k)} = c \ln(\phi_*/\phi) \tag{43}$$

$$\Delta N(k) \equiv N_{\rm COBE} - N(k) \equiv \ln(k/k_{\rm COBE}), \tag{44}$$

where s is an integration constant.[9] Equation (5) then gives

$$\frac{n(k)-1}{2} = s e^{c\Delta N(k)} - c. \tag{45}$$

Some lines of fixed $n_{\rm COBE}$ in the plane s versus c are shown in the left-hand panel of Fig. 3. In order to evaluate Eq. (26), we also need the variation of δ_H which comes from integrating this expression,

$$\frac{\delta_H(k)}{\delta_H(k_{\rm COBE})} = \exp\left[\frac{s}{c}(e^{c\Delta N} - 1) - c\Delta N\right]. \tag{46}$$

We are mostly interested in cosmological scales between $k_{\rm COBE}$ and k_8, corresponding to $0 \lesssim \Delta N \lesssim 4$. In this range the scale-dependence of n is approximately linear (taking $|c| \lesssim 1$) and the variation $\Delta n \equiv n_8 - n_{\rm COBE}$ is given approximately by

$$\Delta n \simeq 4\frac{{\rm d}n}{{\rm d}\ln k} \simeq 8sc. \tag{47}$$

In contrast with the prediction Eqs. (32) and (33) of the earlier models we considered, Δn is positive. Also in contrast with those models, it is not tied to the magnitude of $|n-1|$, and (as we shall see) may be significant even with present data, for physically reasonable values of the parameters. In the right-hand panel of Fig. 3, we show the branches of the hyperbola $8sc = \Delta n$, for the reference value $\Delta n = 0.04$. Within the hyperbola, the scale dependence of n is probably too small to be significant with present data.

The spectral index Eq. (45) depends on the coupling c, which we already discussed, and the integration constant s. To satisfy the slow-roll conditions $M_{\rm P}^2|V''/V| \ll 1$ and $M_{\rm P}^2(V'/V)^2 \ll 1$, both c and s must be at most of order 1 in magnitude. Significant additional constraints on s follow, if we make the reasonable assumptions that the mass continues to run to the end of slow-roll inflation, and that the linear approximation remains *roughly* valid. Indeed, setting ΔN

[9] In an earlier paper [31] we used $\sigma \equiv s e^{cN_{\rm COBE}}$, but s is more convenient.

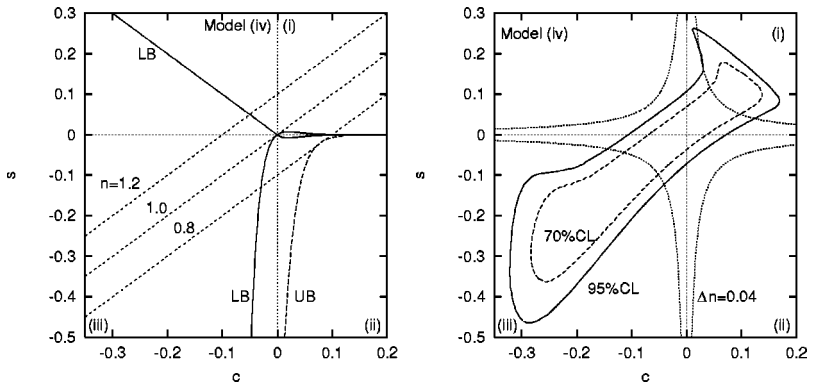

FIG. 3. The parameter space for the running mass model. In the left-hand panel we show the straight lines corresponding to $n_{\rm COBE}=1.2$, 1.0, and 0.8. Also shown in the left-hand panel are the lower bound Eq. (48), the upper bound Eq. (49), and (diagonal line in upper right quadrant) the weak lower bound Eq. (50). [The weak upper bound Eq. (51) is off the scale.] As explained in the text, these curves define the theoretically reasonable region of the parameter space. In the right-hand panel, we show the region allowed by observation, in the case that reionization occurs when $f\simeq 1$. Note that the allowed region is parallel to the fixed n_{COBE} lines around $n_{COBE}\simeq 1$, as one would expect. To show the scale dependence of the prediction for n, we also show in this panel the branches of the hyperbola $8sc=\Delta n\equiv n_8-n_{\rm COBE}$, for the reference value $\Delta n=0.04$.

$=N_{\rm COBE}$, Eq. (43) becomes $s=e^{-cN_{\rm COBE}}c\,\ln(\phi_*/\phi_{\rm end})$. Discounting the possibility that the end of inflation is very fine-tuned, to occur close to the maximum or minimum of the potential, this gives a lower bound

$$|s|\gtrsim e^{-cN_{\rm COBE}}|c|. \tag{48}$$

In the case of positive c [models (i) and (ii)], we also obtain a significant upper bound by setting $\Delta N=N_{\rm COBE}$ in Eq. (45), and remembering that slow-roll requires $|n-1|\lesssim 1$:

$$|s|\lesssim e^{-cN_{\rm COBE}}\quad (c>1). \tag{49}$$

In the simplest case, that slow-roll inflation ends when $n-1$ actually becomes of order 1, this bound becomes an actual estimate, $|s|\sim e^{-cN_{\rm COBE}}$.

In the case of models (i) and (iv), the mass may cease to run before the end of slow-roll inflation (but after cosmological scales leave the horizon, or the running mass model would not apply) at some point $N_{\rm run}$. In this somewhat fine-tuned situation, $N_{\rm COBE}$ in the above estimates should be replaced $N_{\rm COBE}-N_{\rm run}$, which may be much less than $N_{\rm COBE}$. In the case of model (iv), this leads to a weaker lower bound

$$s\gtrsim|c|\quad (c<0). \tag{50}$$

In the case of model (i) it leads to a weaker upper bound

$$s\lesssim 1\quad (c>0). \tag{51}$$

In the left-hand panel of Fig. 3, we show the bounds relevant to the choice of parameter's ranges, i.e. the lower bound Eq. (48), the upper bound Eq. (49) and the weak lower bound Eq. (50).

C. The magnitude of the spectrum

Although it is not directly relevant for our investigation of the spectral index, we should mention the constraint on the running mass model that comes from the observed magnitude $\mathcal{P}_{\mathcal{R}}{}^{1/2}\simeq 10^{-5}$ of the spectrum. From Eq. (1),

$$\frac{4}{25}\mathcal{P}_{\mathcal{R}}=\frac{V_0}{\phi_*^2 M_{\rm P}^2}\exp\left(\frac{2s}{c}\right)\frac{1}{|s|^2}. \tag{52}$$

This prediction involves V_0 and ϕ_*, in addition to the parameters c and s that determine the spectral index.

The simplest thing is to again assume gravity-mediated SUSY breaking, with the ultra-violet cutoff at the traditional scale around $M_{\rm P}$, and the same supersymmetry breaking scale during inflation as in the true vacuum so that $V_0^{1/4}\sim 10^{10}\,$GeV. In this scenario, one expects $|m^2(Q)|\sim V_0/M_{\rm P}^2$ at $Q\sim M_{\rm P}$. As Stewart pointed out in the first paper on the subject, with this very traditional set of assumptions, Eq. (52) can give the correct COBE normalization, with $|c|$ in the physically favored range 10^{-1} to 10^{-2}.[10]

It is remarkable that the most traditional set of assumptions can give a model with the correct COBE normalization, and, as we shall see, with a viable spectral index. If one relaxes these assumptions, there is much more freedom in choosing V_0 and ϕ_*. Such freedom may be very welcome, in coping with the difficulty of implementing inflation in the context of large extra dimensions [34].

D. Observational constraints on the running mass models

Extremizing with respect to all other parameters, we have calculated χ^2 in the s vs c plane and obtained contour levels for χ^2 equal to the minimum value plus 2.41 and 5.99 respectively, corresponding nominally to the 70% and 95%

[10]At the crudest level, one can verify this using the linear approximation Eq. (37) all the way up to the $\phi\sim M_{\rm P}$, corresponding to $\ln(M_{\rm P}/\phi_*)\sim 1/c\sim 10$ to 100. Proper calculations [29–31] using the renormalization group equations (RGE's) lead to the same conclusion.

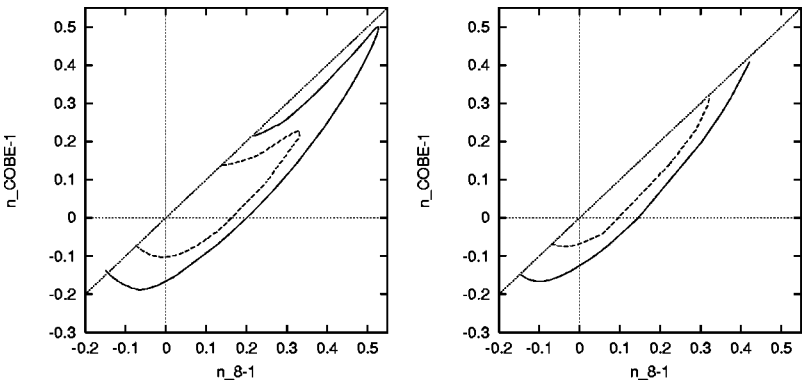

FIG. 4. Allowed region in the $n_{\rm COBE}-1$ vs n_8-1 plane at 95% C.L. (solid line) and 70% C.L. (dashed line) for positive s and c [model (i)]. The two panels correspond to different hypotheses about the reionization epoch. In the right panel, it is assumed that reionization occurs when a fraction $f=10^{-2.2}$ of the matter has collapsed into bound structures, while in the left panel the fraction is taken to be $f\sim 1$.

confidence level in two variables. (The χ^2 function presents actually two nearly degenerate minima in the allowed region, one in the positive and one in the negative quadrants [models (i) and (iii)], separated by a very low barrier, but we assume that the usual quadratic estimate of the probability content is not very far from the true value.)

The allowed region is shown in the right-hand panel of Fig. 3, for the case that reionization occurs when $f\simeq 1$. For $c=0$ or $s=0$ the constant n result is recovered with $n-1=-2c$ or $2s$; our plots give in this case a slightly larger allowed interval with respect to the two sigma value in the previous section, due to the mismatch between the statistical one variable and two variables 95% C.L. contours. This allowed region is not too different from the one that we estimated earlier [31], by imposing the crude requirement $|n-1|<0.2$ at both the COBE scale and the low scale corresponding to $N_{\rm COBE}-10$. [Note that in the earlier work we used the less convenient variable $\sigma\equiv s\exp(cN_{\rm COBE})$, instead of s.]

The allowed region for models (ii) and (iv) lies inside the hyperbola corresponding to $\Delta n=.04$, which means that their scale-dependence is hardly significant at the level of present data. In contrast, the allowed region for models (i) and (iii) extends to $\Delta n\geqslant 0.2$, representing an extremely significant scale dependence even with present data. To demonstrate this, we show in Figs. 4 and 5 the allowed regions for models (i) and (iii) in the n_8 versus $n_{\rm COBE}$ plane. In the case of model (iii), the theoretical bounds on the parameters restrict the parameter space to a small corner of the allowed region, within which n has negligible variation. In contrast, there is no significant theoretical restriction on the parameters in the case of model (i), and n has significant variation in a physically reasonable regime of parameter space. In both cases, a lower value of the fraction of collapsed matter f just reduces the allowed region at large n, without affecting significantly the allowed scale-dependence of n.

In the case of model (i), a further observational constraint comes from the requirement that the density perturbation on scales leaving the horizon at the *end* of inflation, should be small enough to avoid dangerous black hole formation. The linear approximation is not adequate on such small scales, and one should instead evaluate the running mass using the RGE. The simplest assumption is that the RGE corresponds to a single gauge coupling, either with or without asymptotic freedom [30]. The black hole constraint has been evaluated for these cases [35]. The constraint amounts more or less to an upper bound on $n_{\rm COBE}$, typically in the range 1.1 to 1.3 depending on the choices of $N_{\rm COBE}$ and other parameters. Such a bound significantly reduces the allowed region of parameter space, but still leaves a region where n has a strong variation.

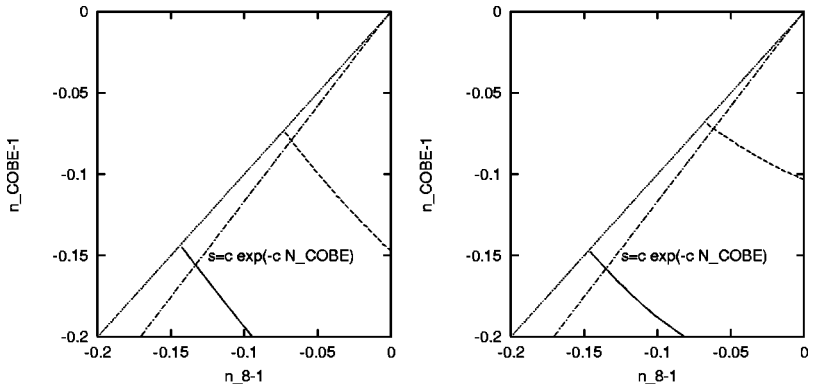

FIG. 5. Allowed region in the $n_{\rm COBE}-1$ vs n_8-1 plane for negative s and c [model (iii)]. Again the two panels correspond to different reionization epoch hypothesis, as in Fig. 4. The allowed region is below the dotted line $n_8=n_{\rm COBE}$, and above the solid (dashed) line at 95% (70%) confidence level. These lines do not depend on the value of $N_{\rm COBE}$. The line $s=ce^{cN_{\rm COBE}}$ is also drawn for $N_{\rm COBE}=50$. The theoretically favored regime $|s|\geqslant|c|e^{cN_{\rm COBE}}$ is the sector between this line and the $n_8=n_{\rm COBE}$ line. The region of positive n_8-1 and/or $n_{\rm COBE}-1$ is not shown, since it corresponds to $|c|\gg|s|e^{-cN_{COBE}}$.

V. CONCLUSION

In the context of the ΛCDM model, we have evaluated the observational constraint on the spectral index $n(k)$. This constraint comes from a range of data, including the height of the first peak in the CMB anisotropy, which we take to be 80 ± 10 μK (nominal 1-σ). Reionization is assumed to occur when some fixed fraction f of the matter collapses, and the most important results are insensitive to this fraction in the reasonable range $10^{-4}\lesssim f\lesssim 1$.

We first considered the case that n has negligible scale dependence, comparing the observational bound with the prediction of various models of inflation. A significant improvement in the 2-σ lower bound, which may well occur with the advent of slightly better measurements of the CMB anisotropy, will become a serious discriminator between models of inflation. Even the present bound has serious implications if, as is very possible, late-time gravitino creation or some other phenomenon requires an era of thermal inflation after the usual inflation.

We also considered the running mass models of inflation, where the spectral index can have significant scale dependence. Because of this scale dependence, it is in this case crucial to fix not the epoch of reionization, but the fraction f of matter that has collapsed at that epoch. We presented results for the choice $f=1$ (corresponding to $z_R\simeq 13$ if the spectral index has negligible scale dependence), and for a perhaps more reasonable choice $f=10^{-2.2}$. In the running-mass models, the scale-dependent spectral index $n(k)$ is given by $n-1=s\exp(c\Delta N)-c$, where $\Delta N=\ln(k_{\rm COBE}/k)$. The parameters in this expression can be of either sign, leading to four different models of inflation. Barring fine-tuning, one expects s to be in the range $|c|e^{-cN_{\rm COBE}}\lesssim|s|\lesssim e^{-cN_{\rm COBE}}$. The parameter c depends on the nature of the soft supersymmetry breaking, but in the simplest case of gravity-mediation it becomes a dimensionless coupling strength, presumably of order 10^{-1} to 10^{-2} in magnitude.

Without worrying about the origin of the parameters c and s, we have investigated the observational constraints on them. In the case $c,s>0$ [referred to as model (i)] we find that n can have a significant variation on cosmological scales, with $n-1$ passing through zero signaling a minimum of the spectrum of the primordial curvature perturbation. In a future paper, we shall exhibit the possible effect of this scale dependence on the CMB anisotropy, at and above the first peak.

ACKNOWLEDGMENTS

We thank Pedro Ferreira and Andrew Liddle and Martin White for useful discussions.

[1] M. S. Turner, astro-ph/9904051; W. L. Freedman, Phys. Scr. **T85**, 37 (2000); N. A. Bahcall, J. P. Ostriker, S. Perlmutter, and P. J. Steinhardt, Science **284**, 1481 (1999).
[2] http://imogen.princeton.edu/~page/where_is_peak.html.
[3] P. De Bernardis *et al.*, Nature (London) **404**, 955 (2000).
[4] D. L. Harrison *et al.*, astro-ph/0004357.
[5] S. Hanany *et al.*, astro-ph/0005123.
[6] F. C. van den Bosch and R. A. Swaters, astro-ph/0006048.
[7] A. R. Liddle, D. H. Lyth, P. T. P. Viana, and M. White, Mon. Not. R. Astron. Soc. **282**, 281 (1996).
[8] K. A. Olive, G. Steigman, and T. P. Walker, Phys. Rep. **333-334**, 389 (2000).
[9] S. Sarkar, Rep. Prog. Phys. **59**, 1493 (1996).
[10] P. T. P. Viana and A. R. Liddle, astro-ph/9902245.
[11] W. Sutherland *et al.*, astro-ph/9901189.
[12] http://www.sns.ias.edu/~matiasz/CMBfast/CMBfast.html.
[13] E. F. Bunn and M. White, Astrophys. J. **480**, 6 (1997).
[14] E. F. Bunn, A. R. Liddle, and M. White, Phys. Rev. D **54**, R5917 (1996).
[15] J. A. Peacock, *Cosmological Physics* (Cambridge University Press, Cambridge, England, 1999).
[16] A. R. Liddle and D. H. Lyth, *Cosmological Inflation and Large–Scale Structure* (Cambridge University Press, Cambridge, England, 1999).
[17] A. R. Liddle and D. H. Lyth, Mon. Not. R. Astron. Soc. **273**, 1177 (1995). astro-ph/9812125.
[18] M. White, Phys. Rev. D **53**, 3011 (1996).
[19] J. R. Bond and A. H. Jaffe, presented at Discussion Meeting on Large Scale Structure in the Universe, Royal Society, London, 1998, astro-ph/9809043.
[20] B. Novosyadlyj *et al.*, astro-ph/9912511.
[21] A. E. Lange *et al.*, astro-ph/0005004.
[22] A. Balbi *et al.*, astro-ph/0005124.
[23] D. H. Lyth and A. Riotto, Phys. Rep. **314**, 1 (1999).
[24] E. D. Stewart and J. D. Cohn, astro-ph/0002214.
[25] D. H. Lyth and E. D. Stewart, Phys. Rev. D **53**, 1784 (1996).
[26] R. Kallosh, L. Kofman, A. Linde, and A. Van Proeyen, Phys. Rev. D **61**, 103503 (2000); G. F. Giudice, I. Tkachev, and A. Riotto, J. High Energy Phys. **08**, 009 (1999); D. H. Lyth, Phys. Lett. B **469**, 69 (1999); hep-ph/9911257.
[27] D. H. Lyth, Phys. Lett. B **476**, 356 (2000); hep-ph/0003120.
[28] E. D. Stewart, Phys. Lett. B **391**, 34 (1997).
[29] E. D. Stewart, Phys. Rev. D **56**, 2019 (1997).
[30] L. Covi, D. H. Lyth, and L. Roszkowski, Phys. Rev. D **60**, 023509 (1999).
[31] L. Covi and D. H. Lyth, Phys. Rev. D **59**, 063515 (1999).
[32] L. Covi, Phys. Rev. D **60**, 023513 (1999).
[33] G. German, G. Ross, and S. Sarkar, Phys. Lett. B **469**, 46 (1999).
[34] See, for instance, D. H. Lyth, Phys. Lett. B **466**, 85 (1999).
[35] S. M. Leach, I. J. Grivell, and A. R. Liddle, Phys. Rev. D **62**, 043516 (2000).